



**Cell Surface ABP1-TMK Auxin-Sensing Complex Activates ROP
GTPase Signaling**
Tongda Xu *et al.*
Science **343**, 1025 (2014);
DOI: 10.1126/science.1245125

This copy is for your personal, non-commercial use only.

If you wish to distribute this article to others, you can order high-quality copies for your colleagues, clients, or customers by [clicking here](#).

Permission to republish or repurpose articles or portions of articles can be obtained by following the guidelines [here](#).

The following resources related to this article are available online at www.sciencemag.org (this information is current as of February 28, 2014):

Updated information and services, including high-resolution figures, can be found in the online version of this article at:

<http://www.sciencemag.org/content/343/6174/1025.full.html>

Supporting Online Material can be found at:

<http://www.sciencemag.org/content/suppl/2014/02/26/343.6174.1025.DC1.html>

This article **cites 39 articles**, 13 of which can be accessed free:

<http://www.sciencemag.org/content/343/6174/1025.full.html#ref-list-1>

This article appears in the following **subject collections**:

Botany

<http://www.sciencemag.org/cgi/collection/botany>

provides a localized assessment of mast cell responses, maintaining the factor of 100 times the 2NP concentration relative to that of DNP. At 30 min after exposure to DNP or 2NP, vascular permeability as measured by extravasation of Evans blue dye (see supplementary materials) was significantly higher in DNP- than 2NP-treated mice (fig. S6A). Consistent with this result, more mast cells were degranulated in animals treated with DNP. Ear swelling was significantly different 30 min after DNP or 2NP treatment but narrowed with time (fig. S6B), and the increase in the thickness of the dermis was similar at 3 hours after stimulation (fig. S6C). Immune cell infiltration was similarly increased in animals exposed to DNP or 2NP (fig. S6D). By 12 hours after stimulation, the thickness of the dermis returned to that of control mice (fig. S6E) but immune cell infiltrates were still elevated relative to control mice (fig. S6F). Given that an inflammatory response was initiated by either DNP or 2NP, we explored the cell types involved. Gr-1⁺ CD11c⁻ CD11b⁺ cells were distinguished on the basis of the myeloid marker 7/4 [Ly-6B.2, which is somewhat more highly expressed by recently generated inflammatory macrophages (20)] from neutrophils as marked by Ly-6G (Fig. 4A). Exposure to DNP caused increased numbers of neutrophils relative to inflammatory macrophages, whereas this ratio was reversed in animals treated with 2NP, consistent with the increased secretion of monocyte-

or macrophage-attracting chemokines, such as CCL2, CCL3, and CCL4, after treatment of mast cells with 2NP (Fig. 1D). Whole-mount immunohistochemical analysis of the skin also revealed these differences (Fig. 4, B and C), and skin mast cells from 2NP-treated mice produced greater amounts of CCL2 than did those in the skin of DNP-treated mice (fig. S7). Thus, low-affinity stimulation of FcεRI results in an inflammatory response marked by a shift in the monocyte or macrophage/neutrophil ratio.

Collectively, our findings demonstrate that differences in the affinity of antigen and antibody interactions are discriminated by receptors through qualitative changes in molecular signals resulting in distinct outcomes. This discriminatory ability of receptors may extend beyond the immune system.

References and Notes

- H. G. Dohlman, J. W. Thorner, *Annu. Rev. Biochem.* **70**, 703–754 (2001).
- M. Behar, N. Hao, H. G. Dohlman, T. C. Elston, *PLoS Comput. Biol.* **4**, e1000197 (2008).
- J. P. Kinet, *Annu. Rev. Immunol.* **17**, 931–972 (1999).
- S. J. Galli, M. Tsai, A. M. Piliponsky, *Nature* **454**, 445–454 (2008).
- C. Isersky, J. Rivera, S. Mims, T. J. Triche, *J. Immunol.* **122**, 1926–1936 (1979).
- H. Metzger, *J. Immunol.* **149**, 1477–1487 (1992).
- N. L. Andrews *et al.*, *Immunity* **31**, 469–479 (2009).
- U. Blank, J. Rivera, *Trends Immunol.* **25**, 266–273 (2004).

- D. R. Jackola, L. K. Pierson-Mullany, C. L. Liebler, M. N. Blumenthal, A. Rosenberg, *Mol. Immunol.* **39**, 367–377 (2002).
- C. Torigoe, J. K. Inman, H. Metzger, *Science* **281**, 568–572 (1998).
- E. Razin, *Methods Enzymol.* **187**, 514–520 (1990).
- C. R. Monks, B. A. Freiberg, H. Kupfer, N. Sciaky, A. Kupfer, *Nature* **395**, 82–86 (1998).
- A. Grakoui *et al.*, *Science* **285**, 221–227 (1999).
- V. Parravicini *et al.*, *Nat. Immunol.* **3**, 741–748 (2002).
- M. Vig *et al.*, *Nat. Immunol.* **9**, 89–96 (2008).
- A. M. Gilfillan, J. Rivera, *Immunol. Rev.* **228**, 149–169 (2009).
- H. Hong *et al.*, *Blood* **110**, 2511–2519 (2007).
- G. Gomez *et al.*, *J. Immunol.* **175**, 7602–7610 (2005).
- J. H. Lee *et al.*, *J. Immunol.* **187**, 1807–1815 (2011).
- M. Rosas, B. Thomas, M. Stacey, S. Gordon, P. R. Taylor, *J. Leukoc. Biol.* **88**, 169–180 (2010).

Acknowledgments: Supported by the intramural research program of the National Institute of Arthritis and Musculoskeletal and Skin Diseases and by its Laboratory Animal Care and Use Section and Flow Cytometry Group, Office of Science and Technology. All data are provided in the main paper and supplementary materials. The authors declare no conflicts of interest.

Supplementary Materials

www.sciencemag.org/content/343/6174/1021/suppl/DC1
Materials and Methods

Figs. S1 to S7
Movies S1 to S6
References (21–34)

8 October 2013; accepted 17 January 2014
Published online 6 February 2014;
10.1126/science.1246976

Cell Surface ABP1-TMK Auxin-Sensing Complex Activates ROP GTPase Signaling

Tongda Xu,^{1,2,3} Ning Dai,^{4*} Jisheng Chen,¹ Shingo Nagawa,^{1,3} Min Cao,² Hongjiang Li,^{1,5,6} Zimin Zhou,² Xu Chen,^{5,6} Riet De Rycke,⁵ Hana Rakusová,^{5,6} Wuyi Wang,^{3,7†} Alan M. Jones,⁸ Jiří Friml,^{5,6,9} Sara E. Patterson,⁷ Anthony B. Blecker,^{4‡} Zhenbiao Yang^{1,3,10§}

Auxin-binding protein 1 (ABP1) was discovered nearly 40 years ago and was shown to be essential for plant development and morphogenesis, but its mode of action remains unclear. Here, we report that the plasma membrane–localized transmembrane kinase (TMK) receptor–like kinases interact with ABP1 and transduce auxin signal to activate plasma membrane–associated ROPs [Rho-like guanosine triphosphatases (GTPase) from plants], leading to changes in the cytoskeleton and the shape of leaf pavement cells in *Arabidopsis*. The interaction between ABP1 and TMK at the cell surface is induced by auxin and requires ABP1 sensing of auxin. These findings show that TMK proteins and ABP1 form a cell surface auxin perception complex that activates ROP signaling pathways, regulating nontranscriptional cytoplasmic responses and associated fundamental processes.

Auxin regulates nearly all aspects of plant development and behavior and impinges on a great variety of responses involving cell polarization, expansion, division and differentiation. Exactly how this small-molecule hormone achieves this multitude of diverse roles is largely unexplained, although it may be perceived by multiple functionally distinct auxin perception and signaling systems (1–6). Members of the nu-

clear TIR1/AFB F-box protein auxin receptor and AUX/IAA co-receptor families modulate nuclear gene transcription in response to various auxin concentrations (1–4).

Independently of the TIR1 family, auxin-binding protein 1 (ABP1) was proposed to perceive extracellular auxin to regulate a plethora of plasma membrane or cytoplasmic responses not necessarily involving gene transcription (6–18).

ABP1 may also coordinate with the TIR1/AFB pathway to regulate gene transcription (16, 19). ABP1 is essential for early embryogenesis, root development, leaf expansion, cell morphogenesis, and subcellular distribution of PIN auxin transporters (6, 8, 9, 12, 13, 15–18, 20, 21). ABP1 is required for the auxin-dependent activation of ROPs [Rho-like guanosine triphosphatases (GTPases) from plants] at the plasma membrane,

¹Center for Plant Cell Biology, Department of Botany and Plant Sciences, University of California, Riverside, CA 92521, USA.

²Temasek Life Sciences Laboratory, 1 Research Link, National University of Singapore, 117604 Singapore. ³Shanghai Center for Plant Stress Biology, Shanghai Institutes for Biological Sciences, The Chinese Academy of Sciences, Shanghai 200032, China.

⁴Department of Botany, University of Wisconsin, Madison, WI 53706, USA. ⁵Department of Plant Systems Biology, VIB and Department of Plant Biotechnology and Bioinformatics, Ghent University, 9052 Gent, Belgium. ⁶Bertalanffy Foundation Building, Institute of Science and Technology Austria, Am Campus 1, 3400 Klosterneuburg, Austria. ⁷Department of Horticulture, University of Wisconsin, Madison, WI 53706, USA. ⁸Departments of Biology and Pharmacology, University of North Carolina, Chapel Hill, Chapel Hill, NC 27599, USA. ⁹Mendel Centre for Plant Genomics and Proteomics, Masaryk University, CEITEC MU, CZ-625 00 Brno, Czech Republic. ¹⁰Shanghai Institute of Plant Physiology and Ecology, Shanghai Institutes for Biological Sciences, The Chinese Academy of Sciences, Shanghai 200032, China.

*Present address: Department of Molecular Biology, Massachusetts General Hospital, Boston, MA 02114, USA. †Present address: Ceres, 1535 Rancho Conejo Boulevard, Thousand Oaks, CA 91320, USA.

‡Deceased. §Corresponding author. E-mail: yang@ucr.edu

which subsequently regulates cytoskeletal organization and clathrin-mediated endocytosis of PIN proteins (5, 17, 18, 22, 23). However, it is not known how ABP1 transmits the auxin signal to regulate these cytoplasmic responses. Here, we demonstrate that the transmembrane kinase (TMK) members of the receptor-like kinase family interact with ABP1 on the cell surface in an auxin-dependent manner and are required for the auxin-mediated activation of ROP GTPase signaling.

To transduce extracellular auxin to the cytoplasmic responses, secreted ABP1 is expected to communicate with the cytoplasm through a transmembrane docking protein (17, 18, 24). We hypothesized that TMKs serve as ABP1 docking proteins. TMKs belong to a clade of receptor-like kinases with four functionally overlapping members whose founding member is TMK1. They contain an intracellular kinase domain, a single transmembrane pass, and an extracellular domain with two regions of leucine-rich repeats (LRRs) separated by a non-LRR region. TMKs affect multiple auxin-mediated processes (25). We found that *tmk* mutants are affected in the same responses regulated by ABP1. The *tmk1^{-/-};tmk2^{+/+};tmk3^{+/+};tmk4^{+/+}* mutant (*tmk1^{-/-};tmk234*) displayed embryo lethality, though with a lower penetrance of lethality as conferred by *abp1* null mutations (fig. S1). Both *tmk1^{-/-};tmk234* and *tmk1^{-/-};tmk234* seedlings displayed single cotyledons and fused leaf-cups, typically found in *pin1-1* mutants (Fig. 1, A to C; fig. S2A; and table S1). Some PINs (including PIN1) modulate auxin efflux, are polarly distributed to the plasma membrane, and are regulated by ABP1- and ROP GTPase-dependent auxin signaling (17, 18, 26–28). PIN1 localization is also affected in *tmk1^{-/-};tmk234* mutant (fig. S1, E to G), as in *abp1* or *rop* mutants (18, 28). A weak *abp1* allele (*abp1-5*) greatly enhances cotyledon defects in *tmk1^{-/-};tmk234*, suggesting a functional interaction between ABP1 and TMKs (table S1).

Auxin promotes the development of interdigitated pavement cells in the *Arabidopsis* leaf epidermis through ABP1 and ROP GTPases (18). The pavement cells of *tmk1^{-/-};tmk234* showed interdigitation defects similar to but stronger than those observed in the *abp1-5* mutant (Fig. 1, D and F). Just as in *abp1-5*, the pavement cell defects in *tmk1^{-/-};tmk234* mutants were not rescued by auxin (Fig. 1, D to G) (18). The *abp1-5;tmk1^{-/-};tmk234* quintuple mutant displayed a phenotype similar to that of the *tmk1^{-/-};tmk234* mutant (fig. S2C). These results suggest that TMKs are required for auxin promotion of pavement cell interdigitation and support an overlapping function with ABP1 in this process.

Auxin activates both the ROP2- and ROP6-dependent pathways in an ABP1-dependent manner in leaf pavement cells (18). We determined whether TMKs were also required for the rapid activation of ROP2 and ROP6 GTPases by auxin, similar to ABP1 (18). Green fluorescent protein (GFP)–ROP2 and GFP–ROP6 transgenic plants were crossed with the *tmk1^{-/-};tmk234* mutant, and *tmk1^{-/-};tmk234* plants containing GFP–ROP2 or

–ROP6 were isolated for ROP activity assays (Fig. 2, A to D) (see supplementary materials and methods). In GFP–ROP2 and GFP–ROP6 transgenic lines, the amount of active GFP–ROP2 and GFP–ROP6 proteins increased nearly fourfold upon treatment with 100 nM naphthaleneacetic acid (NAA), as previously shown (Fig. 2, A to D) (18). However, in *tmk1^{-/-};tmk234;GFP–ROP2* or *tmk1^{-/-};tmk234;GFP–ROP6* mutants, auxin-mediated activation of GFP–ROP2 and GFP–ROP6 was largely abolished (Fig. 2, A to D), as in the *abp1-5* mutant (18).

We next assessed the effect of *tmk* mutations on ROP2 and ROP6 signaling targets in leaf pavement cells. The ROP2 effector RIC4, localized to the plasma membrane especially at the tip of the lobes, promotes the accumulation of cortical actin microfilaments (F-actin) (Fig. 2E) (18, 22, 23). In the *tmk1^{-/-};tmk234* mutant, the lobe tip and plasma membrane distribution of GFP–RIC4 was abolished, as in *abp1-5* and *rop2RNAi;rop4-1* mutants (Fig. 2F) (18, 22). Furthermore, cortical F-actin, which normally accumulates at lobe sites (fig. S3A), was absent from the cortical regions of *tmk1^{-/-};tmk234* mutant pavement cells, just as in *abp1-5* mutants (18, 22) (fig. S3B). The ROP6 effector RIC1 associates with cortical microtubules and promotes their organization upon activation by

ROP6. The association of yellow fluorescent protein (YFP)–RIC1 with cortical microtubules was abolished in the *tmk1^{-/-};tmk234* quadruple mutants, causing the disorganization of cortical microtubules, as observed in the *abp1-5* and *rop6-1* mutants (18, 23) (Fig. 2, G to H; and fig. S3, C and D). These results indicate that TMKs participate in auxin perception or signaling that activates both the ROP2 and ROP6 pathways in leaf pavement cells, similar to ABP1.

Given the occurrence of both ROP2 and ROP6 activation at the plasma membrane (18, 22, 23), their upstream signaling components are expected to localize to the cell surface as well. In both the leaf pavement cells and mesophyll cells of a *pTMK1::TMK1-GFP* transgenic line, TMK1-GFP was localized to the plasma membrane (fig. S4, A and B; and fig. S2, H and I). Although ABP1 is mostly found in the endoplasmic reticulum (ER), a fraction of ABP1 was observed on the cell surface in maize (8, 10, 11, 24, 29, 30). To determine ABP1 distribution, we performed immunogold histochemistry in conjunction with transmission electron microscopy (TEM) (fig. S5, B to H) and epifluorescence microscopy of GFP-tagged ABP1 (fig. S5I). The TEM analysis indicates that the majority of ABP1 localized to the ER, whereas ~22% ABP1 is detected on the plasma membrane in *Arabidopsis* root cells,

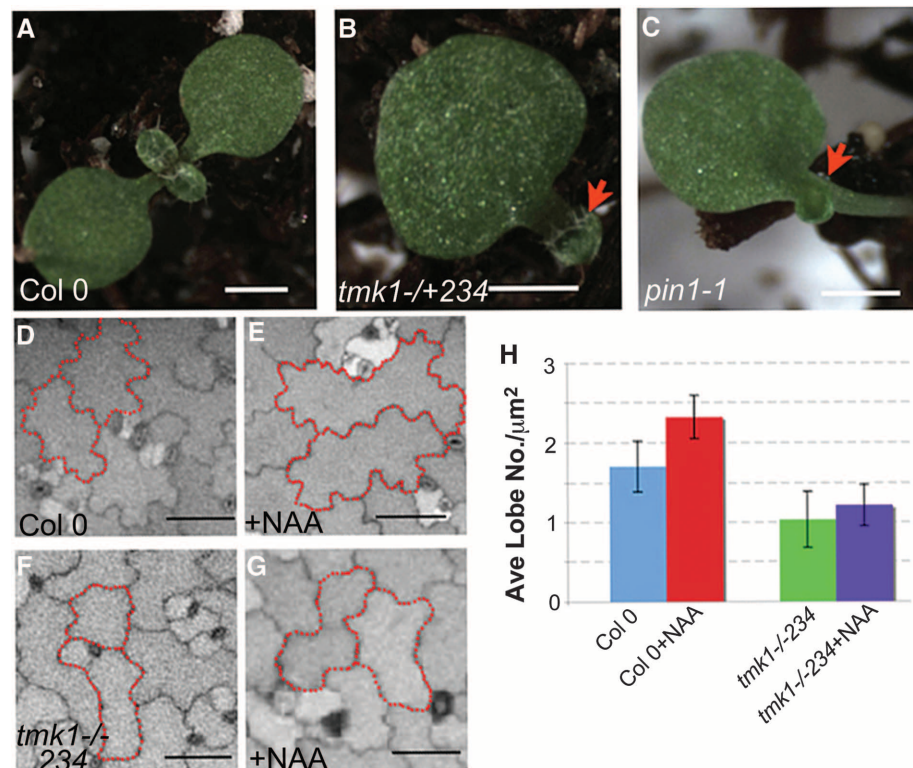


Fig. 1. Transmembrane kinase genes are required for auxin-mediated pavement cell interdigitation. (A to C) The cotyledon phenotype in the wild type (A), *tmk1^{-/-};tmk234* mutant (B), and *pin1-1* mutant (C). Scale bars, 500 μm . (D to H) Pavement cell phenotype of the wild type with (D) or without (E) auxin (20 nM NAA) treatment, and *tmk1^{-/-};tmk234* quadruple mutant with (F) or without (G) auxin (20 nM NAA) treatment. Scale bars, 10 μm . The degree of pavement cell interdigitation was quantified by determining the average number of lobes per square micrometer of pavement cells (Ave Lobe No./ μm^2) (H). Error bars indicate SD.

consistent with ABP1 distribution in maize. ABP1-GFP was found both in the ER and on the plasma membrane in *Arabidopsis* pavement cells (fig. S5J). When these cells were plasmolyzed to detach the plasma membrane from the cell wall, ABP1 signal was observed in strands connecting the apoplast and the plasma membrane (fig. S5I). As a negative control, cytoplasmic dominant-negative ROP2 and ER-localized Calnexin did not show comparable apoplastic signal (fig. S5, K and L). These results support the hypothesis that TMK1 and ABP1 are localized to the cell surface suitably for the activation of ROP2 and ROP6.

Our data suggest that TMKs and ABP1 are both required for the activation of plasma membrane-localized ROP2 and ROP6 GTPases in leaf pavement cells (Fig. 2) (18). In addition, plasma membrane-localized TMKs are required for cell expansion in several other cell types, including mesophyll cells (fig. S2I) (25). ABP1 is also known to promote cell expansion in mesophyll cells; in particular, the cell surface-localized ABP1

has been implicated in the promotion of auxin-mediated expansion of mesophyll cells (12, 13). Thus, we hypothesized that secreted ABP1 and the plasma membrane-localized TMK1 physically form a complex in the perception and signaling of extracellular auxin. To test this, we used an antibody to GFP (anti-GFP) to immunoprecipitate the TMK1-GFP protein complex from the protoplasts of *pTMK1::TMK1-GFP* transgenic plants, which were isolated from expanding leaves and contained both mesophyll cells (92%) and epidermal cells (8%). The ABP1 antibody was used to detect the presence of ABP1 in the complex. ABP1 was detected in the TMK1-GFP protein complex but not in the control BR11-GFP immunoprecipitates, indicating that ABP1 specifically associates with the TMK1 protein complex (Fig. 3A). Treatments with auxin NAA or IAA increased the amount of ABP1 detected in the TMK1-GFP protein complex (Fig. 3A). The auxin dosage response was similar to that for the activation ROP2 and ROP6 (18). Furthermore,

the chosen range of concentrations was between 0.2 and 2 times the dissociation constant of NAA binding to ABP1 (7). In a reciprocal experiment using the ABP1 antibody to immunoprecipitate the ABP1 protein complex, we also found that auxin treatment increased the amount of TMK1 protein in this complex (Fig. 3B). These results demonstrate that auxin promotes the formation of the ABP1-TMK1 protein complex.

We next assessed whether auxin promotion of the ABP1-TMK1 complex formation involves ABP1 perception of auxin using the ABP1-5 mutant protein. The *abp1-5* point mutation in the auxin-binding pocket of ABP1 greatly reduces its sensitivity to auxin for the activation of ROP2 and ROP6 (18). Anti-ABP1 detected the ABP1-5 mutant protein in the TMK1 complex only after extended exposure, suggesting that the ABP1-5 mutant protein is, at best, weakly associated with TMK1 (fig. S6, A and B). Moreover, auxin (both NAA and IAA) treatment only weakly enhanced the association of the ABP1-5 mutant protein with the TMK1 complex (Fig. 3C and fig. S6, A and B). These results indicate that ABP1 sensing of auxin is important for the ABP1-TMK1 complex formation.

On the basis of the above results, we propose that the secreted form of ABP1 associates with the extracellular domain of TMK1 at the cell surface. If the extracellular domain associates with ABP1, overexpression of truncated TMK1 (EX-TMK1, AA1-520), in which the intracellular domain is deleted, would act as a dominant-negative mutant (DN-TMK1) by trapping ABP1 and compromising the function of ABP1 and endogenous TMKs. The 35S::EX-TMK1 construct induced a similar pavement cell phenotype to that of *tmk1^{-/-};tmk234* and *abp1-5* mutants (fig. S7, A and B). Furthermore, EX-TMK1 partially or totally blocked the activation of ROP6 and ROP2 by IAA treatment (fig. S7C).

We next tested the physical interaction between ABP1 and EX-TMK1 coexpressed in *Nicotiana benthamiana* tobacco leaves. Coimmunoprecipitation showed that ABP1 associated with both TMK1 and EX-TMK1 fused with HPB (HA-PreScission-Biotin; HA, GE Healthcare Life Sciences) in tobacco leaves (Fig. 4A). The kinase domain, a mutant with the N-terminal LRR repeats removed, or HPB alone did not associate with ABP1 (fig. S6C). ABP1 appeared to immunoprecipitate a greater amount of EX-TMK1 compared with full-length TMK1. Furthermore, the interaction between ABP1 and EX-TMK1 was induced by NAA or IAA in a concentration-dependent manner, very similar to that observed for the association of ABP1 with TMK1-GFP in *Arabidopsis* (Fig. 4A). Finally, the ABP1-5 mutant protein interacted weakly with EX-TMK1-HPB, and the interaction was not promoted by the addition of NAA or IAA (Fig. 4B). Therefore, auxin mediates the interaction between ABP1 and the extracellular domain of TMK1.

Our findings demonstrate that the plasma membrane-localized TMK1 receptor-like kinase

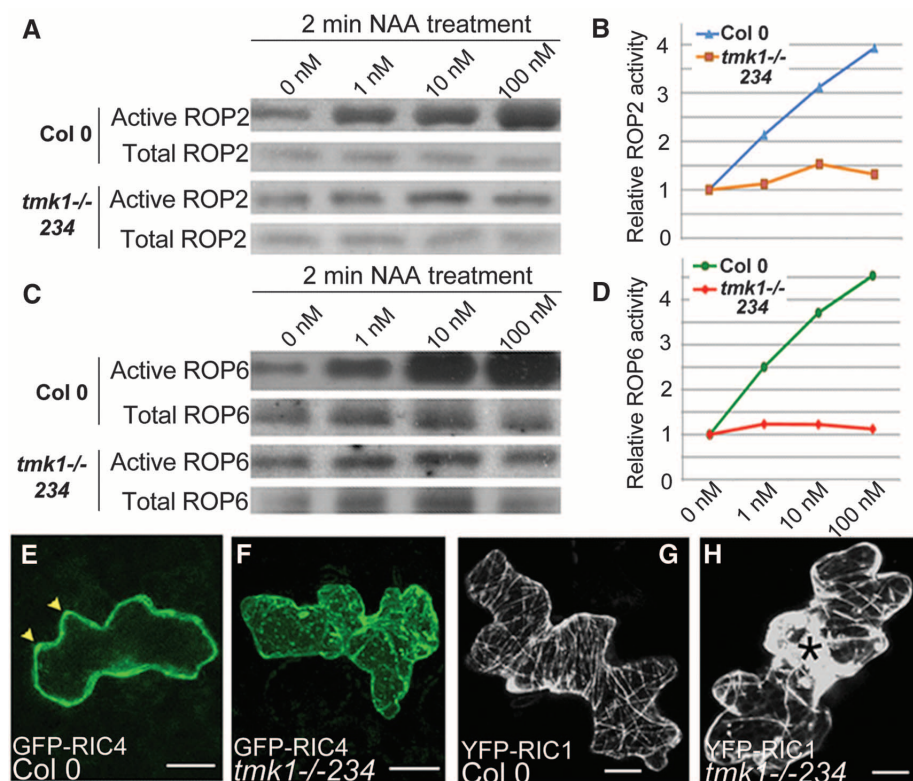


Fig. 2. Transmembrane kinases are required for the auxin-mediated activation of ROP2 and ROP6. (A and B) ROP2 activation by auxin in the wild type and the *tmk1^{-/-};tmk234* mutant was analyzed by pull-down assay, as described previously (18) (A). Quantification of relative active GFP-ROP2 level (amount of GTP-bound GFP-ROP2 divided by amount of total GFP-ROP2) to control (as “1”) is shown (B). ROP6 activation by auxin in the wild type and the *tmk1^{-/-};tmk234* mutant was tested (C) and quantified (D) as above. Data shown represent one of the three replicates. (E to H) The activation of ROP2 was analyzed by using GFP-RIC4 subcellular distribution in the wild type (E) and the *tmk1^{-/-};tmk234* mutant (F). The ratio of plasma membrane-localized RIC4 to cytosolic RIC4 decreased from 3.14 ± 0.62 in the wild type to 0.68 ± 0.31 ($n = 30$ cells; $P < 0.001$) in the *tmk1^{-/-};tmk234*, indicating lower ROP2 activity in the mutant. (G and H) The activation of ROP6 was analyzed by using YFP-RIC1 localization in the wild type (G) and the *tmk1^{-/-};tmk234* mutant (H). The microtubule-localized RIC1 (ratio of RIC1 bundle length to cell size) decreased dramatically from $0.92 \pm 0.26 \mu\text{m}^{-1}$ in the wild type to $0.22 \pm 0.12 \mu\text{m}^{-1}$ ($n = 30$ cells; $P < 0.001$) in the *tmk1^{-/-};tmk234* mutant, indicating lower ROP6 activity level in the mutant. Scale bars, 5 μm .

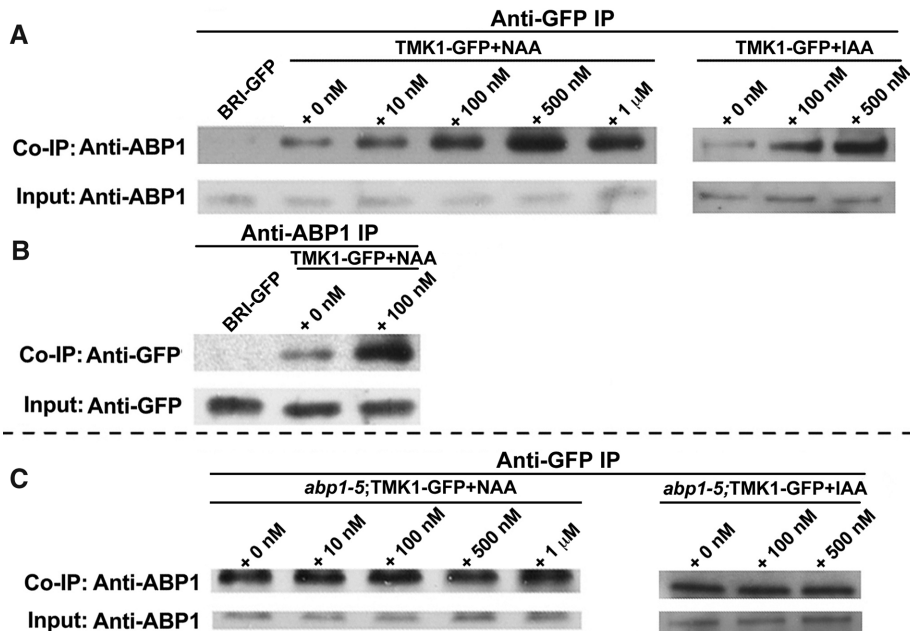


Fig. 3. Auxin promotes the association of TMK1 with ABP1 in *Arabidopsis*. (A and B) The association of ABP1 with TMK1-GFP in *Arabidopsis* leaves was determined by coimmunoprecipitation (Co-IP) assay. Plasma membrane–localized BRI1-GFP was used as a negative control. The protein complex from leaf protoplasts treated with different concentrations of auxin (NAA and IAA) was immunoprecipitated by GFP antibody (A) or ABP1 antibody (B). ABP1 was detected in the TMK1-GFP complex in an auxin-dependent manner (A). TMK1-GFP was detected in the ABP1 complex, also in an auxin-dependent manner (B). Input ABP1 indicates the total amount of ABP1 in protein samples before coimmunoprecipitation. (C) A weak association of TMK1-GFP with an ABP1-5 mutant protein in the *abp1-5;TMK1-GFP* mutant was not induced by auxin addition. The signal shown here (B) was obtained by extended exposure, compared with that shown in (A) (see fig. S6, A and B).

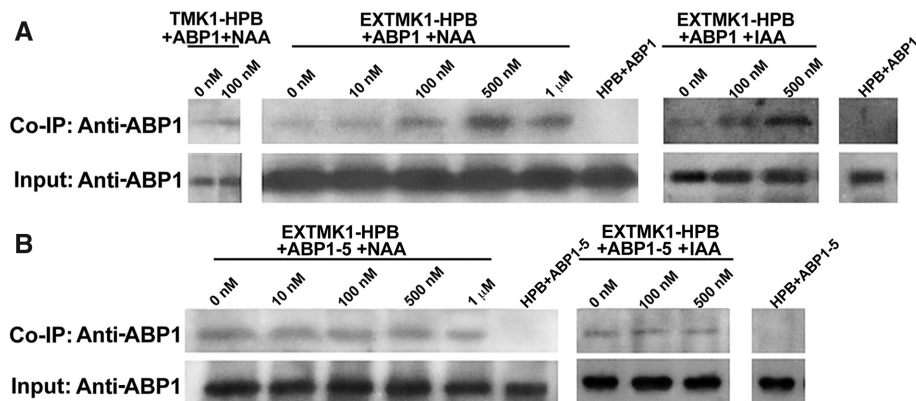


Fig. 4. Auxin promotes the interaction of ABP1 with the extracellular domain of TMK1. (A) The association of ABP1 with TMK1 or EX-TMK1 was analyzed by coimmunoprecipitation in tobacco leaves that transiently expressed ABP1 and EX-TMK1 tagged with HPB. Streptavidin-coated magnetic beads were used to immunoprecipitate TMK1-HPB or EXTMK1-HPB protein complexes, which were immunoblotted with the ABP1 antibody. The same assay was carried out for ABP1-5 and EX-TMK1 (B).

is functionally and physically associated with ABP1 at the cell surface to regulate auxin- and ABP1-mediated activation of ROP GTPase signaling. TMK1 is at least one of the long-sought docking proteins coupling extracellular auxin and its perception by ABP1 to cytoplasmic signaling (6, 14, 24). This discovery solves the mystery of the cell surface–cytoplasmic auxin perception and signaling system and opens up a new hori-

zon in auxin biology. Clearly, the TIR1/AFB-based nuclear pathways are essential for various auxin responses (1, 2). The pleiotropic phenotypes of the *tmk* and *abp1* mutants also indicate an essential role for the extracellular auxin perception (12, 13, 15, 17, 18, 25). The functions of ABP1 and TMKs agree with their role in regulating PIN distribution but also point to unexplored roles for extracellular auxin in other

pathways (6, 17, 18, 21, 26–28). Therefore, the discovery of the ABP1-TMK complex underlies many exciting prospects of elucidating the roles of cell surface auxin perception and its relation with the TIR1/AFB-based nuclear auxin perception.

References and Notes

1. N. Dharmasiri, S. Dharmasiri, M. Estelle, *Nature* **435**, 441–445 (2005).
2. S. Kepinski, O. Leyser, *Nature* **435**, 446–451 (2005).
3. X. Tan *et al.*, *Nature* **446**, 640–645 (2007).
4. K. Mockaitis, M. Estelle, *Annu. Rev. Cell Dev. Biol.* **24**, 55–80 (2008).
5. Z. Yang, *Annu. Rev. Cell Dev. Biol.* **24**, 551–575 (2008).
6. J. H. Shi, Z. B. Yang, *Mol. Plant* **4**, 635–640 (2011).
7. P. M. Ray, U. Dohrmann, R. Hertel, *Plant Physiol.* **59**, 357–364 (1977).
8. A. M. Jones, E. M. Herman, *Plant Physiol.* **101**, 595–606 (1993).
9. A. M. Jones, *Annu. Rev. Plant Physiol. Plant Mol. Biol.* **45**, 393–420 (1994).
10. H. Tian, D. Klämbt, A. M. Jones, *J. Biol. Chem.* **270**, 26962–26969 (1995).
11. S. C. Oliver, M. A. Venis, R. B. Freedman, R. M. Napier, *Planta* **197**, 465–474 (1995).
12. A. M. Jones *et al.*, *Science* **282**, 1114–1117 (1998).
13. J. G. Chen, S. Shimomura, F. Sitbon, G. Sandberg, A. M. Jones, *Plant J.* **28**, 607–617 (2001).
14. G. O. Badescu, R. M. Napier, *Trends Plant Sci.* **11**, 217–223 (2006).
15. N. Braun *et al.*, *Plant Cell* **20**, 2746–2762 (2008).
16. A. Tromas *et al.*, *PLOS ONE* **4**, e6648 (2009).
17. S. Robert *et al.*, *Cell* **143**, 111–121 (2010).
18. T. Xu *et al.*, *Cell* **143**, 99–110 (2010).
19. A. Tromas *et al.*, *Nat. Commun.* **4**, 2496 (2013).
20. J. G. Chen, H. Ullah, J. C. Young, M. R. Sussman, A. M. Jones, *Genes Dev.* **15**, 902–911 (2001).
21. Y. Effendi, S. Rietz, U. Fischer, G. F. Scherer, *Plant J.* **65**, 282–294 (2011).
22. Y. Fu, Y. Gu, Z. Zheng, G. Wasteneys, Z. Yang, *Cell* **120**, 687–700 (2005).
23. Y. Fu, T. Xu, L. Zhu, M. Wen, Z. Yang, *Curr. Biol.* **19**, 1827–1832 (2009).
24. D. Klämbt, *Plant Mol. Biol.* **14**, 1045–1050 (1990).
25. N. Dai, W. Wang, S. E. Patterson, A. B. Bleecker, *PLOS ONE* **8**, e60990 (2013).
26. X. Chen *et al.*, *Curr. Biol.* **22**, 1326–1332 (2012).
27. D. Lin *et al.*, *Curr. Biol.* **22**, 1319–1325 (2012).
28. S. Nagawa *et al.*, *PLOS Biol.* **10**, e1001299 (2012).
29. W. Diekmann, M. A. Venis, D. G. Robinson, *Proc. Natl. Acad. Sci. U.S.A.* **92**, 3425–3429 (1995).
30. N. Leblanc *et al.*, *J. Biol. Chem.* **274**, 28314–28320 (1999).

Acknowledgments: We are grateful to X. Chen, N. Raikhel, V. Gonehal, and members of the Yang laboratory for their stimulating discussion and critical comments on this manuscript. This work is supported by grants from the U.S. National Institute of General Medical Sciences to Z.Y. (GM081451) and A.M.J. (GM065989), the European Research Council (project ERC-2011-StG-20101109-PSDP) and CEITEC – Central European Institute of Technology (CZ.1.05/1.1.00/02.0/068) to J.F., and University of Wisconsin HATCH support to S.E.P. Requests for *tmk* mutant seeds described in this work must be sent to N.D. (ning@molbio.mgh.harvard.edu). Predoctoral fellowship from the Agency for Innovation by Science and Technology (IWT) to H.R.

Supplementary Materials

www.sciencemag.org/content/343/6174/1025/suppl/DC1
Materials and Methods
Supplementary Text
Figs. S1 to S7
Table S1
References (31–39)

26 August 2013; accepted 27 January 2014
10.1126/science.1245125